Pulsed channel flow in Bhutan

L. S. HOLLISTER[1] & D. GRUJIC[2]

[1]*Department of Geosciences, Princeton University, Princeton, New Jersey 08544, USA (e-mail: linc@princeton.edu)*

[2]*Department of Earth Sciences, Dalhousie University, Halifax, Nova Scotia, Canada B3H 4J1*

Abstract: We summarize our results from Bhutan and interpret the Greater Himalaya Sequence (GHS) of Bhutan, together with a portion of the underlying Lesser Himalaya Sequence, in the context of recently published channel flow models. For the GHS rocks now exposed in Bhutan the depth for beginning of muscovite dehydration melting (approximately 750°C at 11 kbar) and associated weakening of these rocks is constrained by geobarometry to be at about 35–45 km. The location of initial melting was down-dip and over 200 km to the north of Bhutan. Melt was produced and injected into ductilely deforming metamorphic rocks as they were extruded towards the south between the Main Central Thrust (MCT) and the South Tibetan Detachment zones. The lateral flow of low viscosity rocks at these depths occurred under southern Tibet between 22 Ma and 16 Ma. Subsequently, the channel rocks decompressed from 11 to 5 kbar (from 35 km to a depth of 15 km), but maintained high temperatures, between about 16 Ma and 13 Ma. The data from Bhutan are consistent with channel flow models if there were several pulses of channel flow. The first, between 22 and 16 Ma, produced the rock seen in the lower half of the GHS of Bhutan. A second pulse, which is cryptic, is inferred to have led to the uplift and exhumation of the MCT zone. A third, in central Bhutan, is exposed now as the hanging wall of the Kakhtang thrust, an out-of-sequence thrust that was active at 12–10 Ma. The latter two pulses likely broke around a plug at the head of the first pulse that was formed where the melt in the channel had solidified.

The geodynamic models of Beaumont *et al.* (2001, 2004) and Jamieson *et al.* (2004) show that channel flow in the Himalaya was a likely consequence of building the Tibetan Plateau, and exhumation of the channel material was a consequence of focused erosion at the Himalaya front in concert with the channel flow. Jamieson *et al.* (2004) interpret most metamorphic and structural data of the central Himalayas in the context of a basic model called HT-1. We here review data from Bhutan (Fig. 1) that support a model of channel flow for formation of the Greater Himalaya Sequence (GHS). Inconsistencies between the basic model and our data can be rationalized by considering pulses of channel flow rather than the single, spatially and temporally continuous episode of channel flow as used in the basic model.

The basic geodynamic model for the Himalaya calls for steady channel flow of thermally weakened rock in a channel from the Miocene to the present. This weakening is inferred to be due to the onset of melting in the mid- to lower crust; a few per cent of melt in a rock is known to lower the viscosity by several orders of magnitude (Rosenberg & Handy 2005). Because rock within the flowing channel, in comparison to the bounding plates, is relatively weak due to the presence of melt, when this melt solidifies (as leucogranite at about 700°C at 5 kbar; L of Fig. 2) the rock becomes stronger. Thus, the head, or the rheological tip, of the low viscosity portion of the channel is defined by the isotherm for this transition. The channel in the basic geodynamic model flowed from under southern Tibet to under the Himalaya. Under Tibet, the channel includes most of the middle crust, some 30–40 km of a 70 km thick crust. At its southern limit, the model channel narrows as it approaches the mountain front at the southern edge of the Tibetan Plateau. There, focused surface erosion leads to rapid removal of rock and to exposure of the channel as the GHS.

The temperature of the channel is buffered by the presence of melt and solid phases. These phases are leucogranite melt, the remaining reactants of the melt-producing reaction, and other products of mica dehydration of metasedimentary rocks, which are in equilibrium at 11–12 kbar at 750–800°C (muscovite + albite + quartz = aluminium silicate + potassium feldspar + leucogranite melt; Fig. 2). According to the basic model, the sedimentary protolith was entrained in the mid-crust as the Indian plate underthrust Tibet (Jamieson *et al.* 2006). The Indian lower crust and lithospheric mantle were subducted while the Late Proterozoic

From: LAW, R. D., SEARLE, M. P. & GODIN, L. (eds) *Channel Flow, Ductile Extrusion and Exhumation in Continental Collision Zones*. Geological Society, London, Special Publications, **268**, 415–423.
0305-8719/06/$15.00

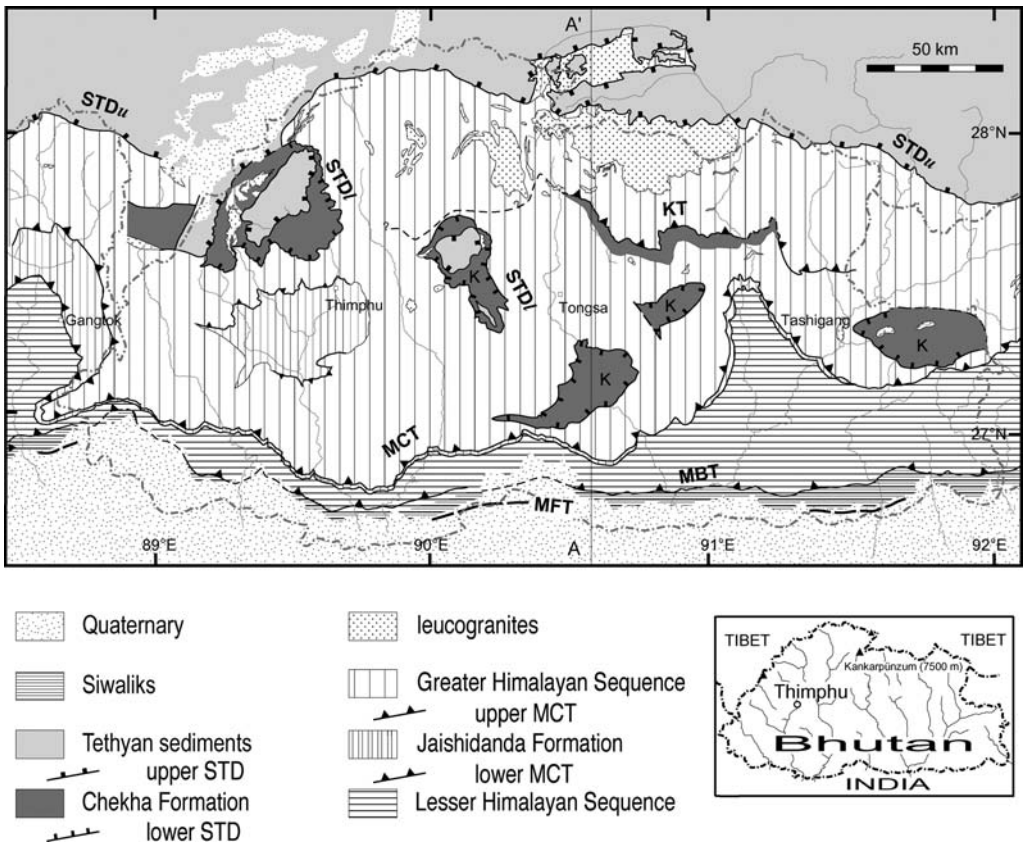

Fig. 1. Geological map of Bhutan and surrounding areas, after Grujic *et al.* (2002) and references therein, with modifications based on continuing mapping by D. Grujic and students, and by Bhutanese colleagues. K, Klippen of Chekha Formation; KT, Kakhtang thrust; MBT, Main Boundary Thrust; MCT, Main Central Thrust; MFT, Main Frontal Thrust; STD, South Tibetan detachment. A–A' indicates line of schematic section in Figure 5.

to Mesozoic sedimentary cover accreted in the middle of the thickening crust. The depth to the resulting channel corresponds to 8–12 kbar. This is the range of maximum model pressures reported from metamorphosed pelitic rocks of the GHS along the entire Himalayan chain (e.g. Brunel & Kienast 1986; Hubbard 1989; Inger & Harris 1992; Macfarlane 1995; Vannay & Hodges 1996; Vannay & Grasemann 1998; Neogi *et al.* 1998; Ganguly *et al.* 2000; Catlos *et al.* 2001; Daniel *et al.* 2003; Dasgupta *et al.* 2004; Harris *et al.* 2004).

We note here that it is exceedingly difficult to extract accurate pressures (and temperatures) from the Himalayan metamorphic rocks. Davidson *et al.* (1997) and Daniel *et al.* (2003) showed that thermobarometry of rocks that are not fully characterized by using X-ray composition maps likely produces unreliable results. This is because of the near-universal chemical disequilibrium due to variable response of mineral compositions to reheating, to decompression at high temperature, and to rapid cooling. Furthermore, the uncertainty due to choice of mineral compositions outweighs analytical or thermodynamic model uncertainties. Accordingly, where, in this paper, we report the pressure in the proposed channel to be 11–12 kbar, we recognize an uncertainty that ranges from 8 to 14 kbar. And we estimate an uncertainty range from 4 to 6 kbar in our reporting of a pressure of 5 kbar. Nevertheless, maximum pressures at peak temperatures reported from the GHS along the Himalaya range only between 8 and 12 kbar.

The 'uniform' pressure of 8–12 kbar is predicted by flow of a subhorizontal channel south from the mid-crust under Tibet. That is, the rocks of the channel do not originate from extreme depths at the base of the Tibetan or Himalayan crust (about 25 kbar). The origin of the GHS rocks from the 'same' depth means that the amount of exhumation depends on how far the channel has progressed

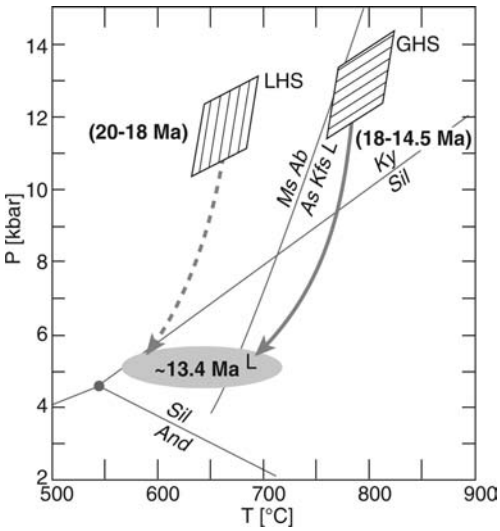

Fig. 2. Pressure–Temperature diagram illustrating P–T estimates from the Greater Himalayan Sequence (GHS) and Lesser Himalayan Sequence (LHS) of Bhutan with respect to phase boundaries taken from Spear *et al.* (1999) and references therein; after Daniel *et al.* (2003). The line labelled MsAb/AsKfsL is the vapour-absent reaction curve muscovite + albite + quartz = aluminium silicate (kyanite or sillimanite) + K-feldspar + liquid (leucogranite melt). L, approximate P–T for solidification of leucogranite.

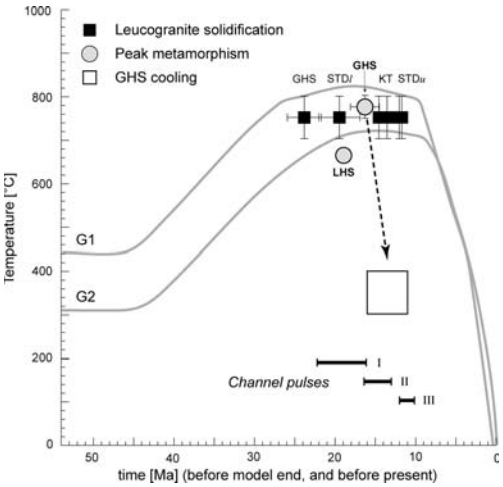

Fig. 3. Comparison between model T–t paths (grey lines) from Jamieson *et al.* (2004, their Fig. 5b) and data from Bhutan. G1 is for a particle that emerges near the base (just above the MCT) of the extruded channel; G2 is for a particle that emerges near the top (just below the STD) of the extruded channel. Leucogranite solidification ages are shown as filled squares; STD*l* is leucogranite that cuts the lower STD (Fig. 1); STD*u* is leucogranite that cuts the upper STD (Fig. 1). All published Ar/Ar and Rb–Sr cooling dates from Bhutan fall within the open square. Arrow illustrates time–temperature cooling path of GHS in Bhutan. The plot shows that cooling ages are older than predicted by the basic geodynamic model (HT1 of Jamieson *et al.* 2004). Peak metamorphic temperatures for the GHS and LHS (Fig. 2) are shown for reference. Time intervals of three proposed pulses of channel flow in central Bhutan are shown by horizontal bars.

laterally towards the Himalayan front, and not on the amount of tectonic uplift.

According to Jamieson *et al.* (2004), if there were continuous flow of the channel from the Miocene to the present, then the rocks of the GHS now exposed at the surface would have passed through the brittle–ductile transition (300–400°C) at 3–5 Ma (Fig. 3). However, the Ar/Ar and Rb–Sr cooling dates on mica, which are set within the temperature range of the ductile–brittle transition, are mainly around 11–16 Ma within the GHS of Bhutan (Fig. 3; Gansser 1983; Castelli & Lombardo 1988; Maluski *et al.* 1988; Ferrara *et al.* 1991; Stüwe & Foster 2001). Jamieson *et al.* (2004) point out that these 'old' cooling dates in the GHS are not predicted by the basic channel flow model, and they suggest several changes to experimental parameters that might account for the discrepancy in cooling temperatures.

The data from Bhutan can be incorporated into the channel flow model if there is an initial pulse of channel flow from 22 Ma to 16 Ma, followed by a second pulse at 16–13 Ma. The first pulse brought the presently exposed GHS into juxtaposition with the Lesser Himalayan Sequence (LHS) at a depth of about 35–45 km, at 16–18 Ma. The second led to rapid exhumation of the GHS along with a portion of the LHS under the Main Central Thrust deformation zone, bringing the entire package to a depth of about 15 km where it cooled rapidly through the Ar/Ar and Rb–Sr closure temperatures of micas. A third pulse, between 12 and 10 Ma, extruded the upper portion of the central Bhutan GHS between the out-of-sequence Kakhtang thrust and a normal shear zone at the top of the GHS (upper STD, Fig. 1). The formation of the North Himalayan gneiss domes (Hodges 2000) is probably temporally associated with this channel pulse. The geodynamic modelling of Beaumont *et al.* (2004) suggests that pulses could occur if the surface erosion is not sufficient to keep pace with the channel propagation and/or if the channel overburden fails. That is, an increase in rate of flow would be caused either by new melt production (weakening) within the channel or by a decrease in surface erosion efficiency (Beaumont *et al.* 2004, figs 12 and 16).

Bhutan data

Five papers, beginning in 1991, trace the development of our understanding of the metamorphic and deformational history of Bhutan (Swapp & Hollister 1991; Grujic *et al.* 1996, 2002; Davidson *et al.* 1997; Daniel *et al.* 2003). This work has its foundation in the classic study of Gansser (1983) and should be viewed in the context of other studies in Bhutan (Maluski *et al.* 1988; Ferrara *et al.* 1991; Bhargava 1995; Edwards *et al.* 1996; Stüwe & Foster 2001; Wiesmayr *et al.* 2002; Carosi *et al.* 2006) and in neighbouring Sikkim and Tibet (Neogi *et al.* 1998; Edwards & Harrison 1997; Ganguly *et al.* 2000; Catlos *et al.* 2004; Dasgupta *et al.* 2004; Harris *et al.* 2004; Searle & Szulc 2005) as well as elsewhere in the Himalayas over the past three decades (reviewed by Hodges 2000).

Guided by the seismic data of Nelson *et al.* (1996) and by the cross-section given by Burchfiel *et al.* (1992), Grujic *et al.* (1996) kept the geometry of the GHS as a wedge between non-parallel walls but modelled the wedge as having deformed ductilely during extrusion, in the presence of melt, thus showing that the earlier concept of a rigid 'slab' did not portray the physical state of the wedge as it extruded. Grujic *et al.* (2002) incorporated the out-of-sequence Kakhtang thrust to reconstruct a much longer channel with parallel walls that extended to 30–40 km depth over a distance of about 200–300 km under the Tibetan Plateau.

According to Grujic *et al.* (1996, 2002), Davidson *et al.* (1997) and Daniel *et al.* (2003), the entire GHS had flowed ductilely towards the south in the presence of melt with the composition of leucogranite. Although the published geological maps convey the impression that leucogranite is present only at the upper structural levels of the GHS, leucogranite dykes and sills, and leucosome pods occur from the Main Central Thrust (MCT) up across the GHS and into the Chekha Formation. The leucosome pods reflect flow of grain boundary melt to extensional zones during ductile deformation (Hollister 1993), and it is the grain boundary melt that weakens the rock (Rosenberg & Handy 2005). Intrusion of dykes and sills during the deformation is documented by textures and progressive deformation of dykes in the presence of liquid. In the middle of deformed dykes, magmatic fabric is preserved that has only a weak solid-state overprint. Fractures of crystals in deformed dykes and sills are filled with melt (Davidson *et al.* 1997). Kyanite relicts in pods and lenses of deformed leucogranite (Fig. 4) show that leucogranite was present early during the south-directed ductile flow. Injection of melt at lower pressures is recorded by the growth of sillimanite near these bodies. Harris & Massey (1994), Harris *et al.* (2004) and Zhang *et al.* (2004) emphasize continuing production of melt during decompression. Kyanite also occurs in leucosomes that were present as melt during the ductile flow (Daniel *et al.* 2003), and in quartz veins in the Jaishidanda Formation below the MCT (Bhargava 1995). Leucogranite dykes cut across the South Tibetan Detachment (STDu and STD1) and are deformed by the top-to-north shear across the STD both in the klippen (Grujic *et al.* 2002) and along the STD near the Tibet–Bhutan border (Burchfiel *et al.* 1992; Edwards *et al.* 1996; Wu *et al.* 1998).

There is general consensus that the leucogranite melts were produced by dehydration melting of a mica-bearing protolith in the core of the orogen (Harris & Massey 1994; Zhang *et al.* 2004). This melting occurs at 750–800°C at 11–12 kbar (Fig. 2), which are the peak metamorphic conditions recorded in the GHS of Bhutan. A necessary condition of channel flow, a substantial drop in rock strength, is achieved due to the weakening effects of partial melt (Hollister & Crawford 1986; Hollister 1993; Rosenberg & Handy 2005). Melt was produced in the GHS between 26 Ma (Thimm *et al.* 1999) and 11 Ma (Edwards & Harrison 1997; Wu *et al.* 1998).

The leucogranite that solidified at the earliest times occurs near the MCT where it was quenched against the cooler, originally greenschist-facies rocks of the footwall. The leucogranite that solidified late in the history of the GHS occurs well within the GHS where Davidson *et al.* (1997) showed that heat from the leucogranite led to development of the lower pressure metamorphic assemblages. Sillimanite also grew as the thrust pile was flattened, and, at the base of the STD, sillimanite grew during top-to-the-north normal-sense shear. Garnet rotated as it grew and was later partially resorbed; sillimanite grew within and along with new garnet on the rims of the earlier garnet (Davidson *et al.* 1997). At the top of the GHS, occurrences of andalusite-bearing leucogranite indicate that, there, leucogranite solidified at lower pressures than those recorded deeper within the GHS.

Daniel *et al.* (2003) showed that the model pressures recorded in garnet schists within a few hundred metres below the MCT, but still within the MCT zone, were the same (Fig. 2; 11–12 kbar at 650°C) as those in the GHS above the MCT where pressures of 11–12 kbar were recorded for kyanite-bearing migmatite at 800°C (Figs 2 & 4). The 11 kbar rocks below the MCT (Fig. 1) are within the Jaishidanda Formation of Bhargava (1995). This zone probably also corresponds to the Lesser Himalayan Crystalline Zone of Grasemann *et al.* (1999) and Vannay *et al.* (2004), or the MCT zone of Lombardo & Rolfo (2000).

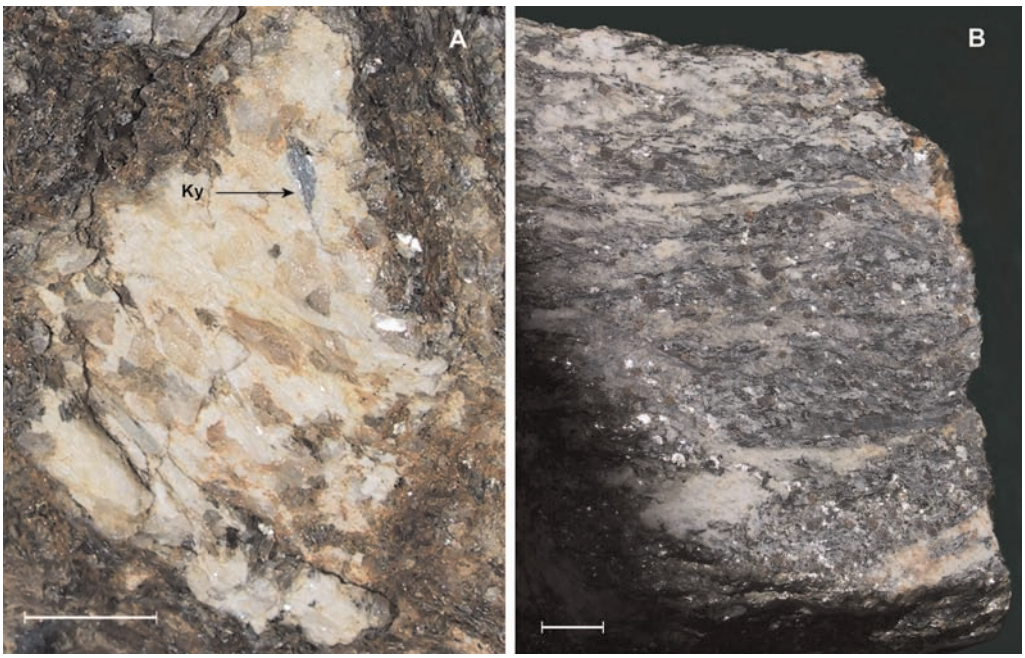

Fig. 4. Photos of deformed pod of leucogranite containing kyanite about 500 m above the MCT, eastern Bhutan. (**a**) Section cut perpendicular to lineation and viewed looking nearly parallel to lineation. (**b**) Surface cut parallel to lineation and perpendicular to foliation. Note that the leucosome pod appears undeformed in the surface perpendicular to the lineation. Scale bars are 1 cm.

Thus, when the MCT was active, the MCT was at a depth corresponding to 11–12 kbar, or 35 km.

Decompression at high temperatures from 11–12 kbar to *c*. 5 kbar (Fig. 2) was recorded by several metamorphic reactions (Davidson *et al.* 1997) including the transition of kyanite-bearing migmatite to sillimanite-bearing migmatite. Locally large differences in peak metamorphic temperature across the GHS existed at the time of decompression (Davidson *et al.* 1997). Intrusion of leucogranite sills and dykes provided some of the heat to locally increase the temperature during decompression (Davidson *et al.* 1997); a solidification date for one of these late sills is 13.4 Ma (Daniel *et al.* 2003). When the ductile flow of the rocks now exposed at the surface ceased, the highest temperature rocks in the hanging wall of the MCT were in the stability field of sillimanite, and pressure had dropped from 11–12 kbar to about 5 kbar. Thus, the rapid exhumation from 11–12 kbar to 5 kbar occurred at high temperature (Fig. 2), and the exhumation post-dated top-to-south penetrative deformation.

The section of the LHS several hundred metres below the MCT is in the greenschist facies (Daniel *et al.* 2003). A major out-of-sequence thrust, the Kakhtang thrust, crosses central Bhutan within the overlying GHS (Fig. 1). The hanging wall of the STD below and south of the Kakhtang thrust (Figs 1 & 5) is composed of the erosional remnants of the Chekha Formation of Bhutan, and it also has greenschist-facies rocks (Grujic *et al.* 2002). Assuming a reasonable geothermal gradient for rapidly exhumed rock, and temperatures for the greenschist facies of 300–450°C, the presence of greenschist-facies rocks above and below the GHS is consistent with both units being at a depth of about 15 km, which is about the same as the depth corresponding to the 5 kbar recorded after decompression of the GHS. The decompression of the GHS to 5 kbar thus included the footwall of the MCT and the hanging wall of the STD.

Detailed field mapping of the GHS rocks showed truncation of isograds within the footwall of the Kakhtang thrust (Davidson *et al.* 1997) and some folding of the footwall rocks. Thus, the portion of the GHS above the Kakhtang thrust represents a portion of the GHS that was extruded from shallower depth at a later time than the underlying portion of the GHS that is now exposed between the Kakhtang thrust and the MCT (Fig. 5).

The hanging wall of the Kakhtang thrust contains higher-temperature migmatites than are present in the footwall (Swapp & Hollister 1991;

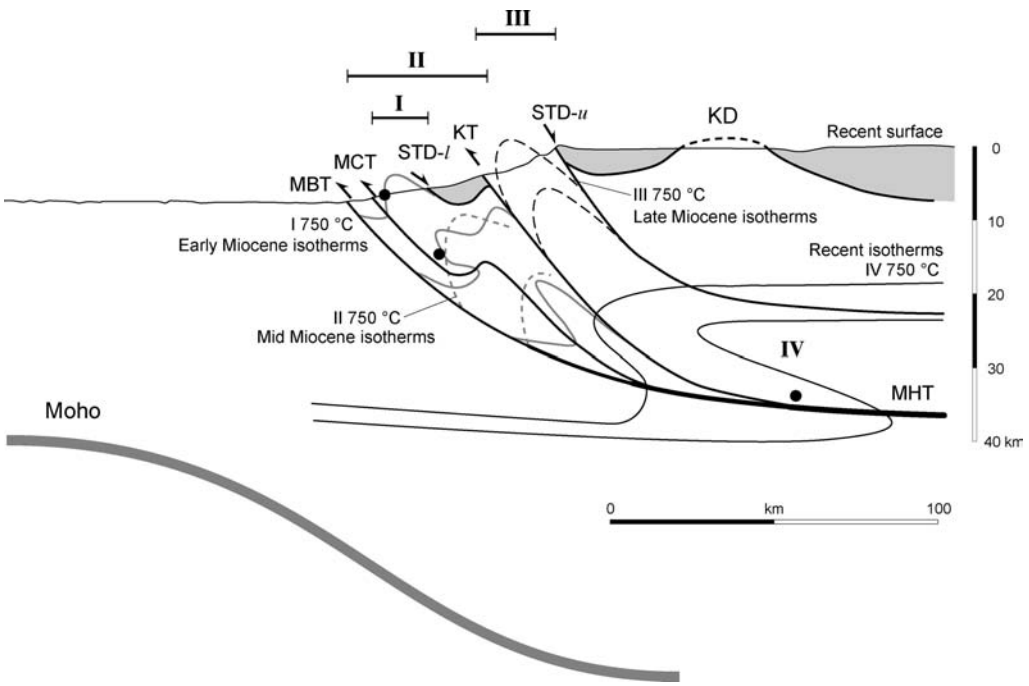

Fig. 5. Schematic cross-section at 90°30' E longitude showing present location of proposed channel pulses. The 750°C isotherms are labeleed according to pulse (I – IV). That for 'Pulse' IV shows inferred position of present isotherm. KT, Kakhtang Thrust; MBT, Main Boundary Thrust; MCT, Main Central Thrust; STD-*l*, lower South Tibetan Detachment (Fig. 1), which, according to our model, was active during Pulse I; STD-*u*, upper STD (Fig. 1), which was active during Pulse III. Large dots show position of kyanite-bearing migmatite (Fig. 4) now at the surface, and where it was following Pulse II (middle dot) and following Pulse I (lower dot). The horizontal bars labelled I, II and III show approximate surface exposure of lower and upper boundaries of the three channels. The upper boundary of Pulse II may have been where the KT is now located, or it may have been the STD-*l*. KD is the Kangmar dome, one of the string of North Himalayan gneiss domes (e.g. Hodges 2000). The locations of the Kangmar dome and STD on the north side of section are based on INDEPTH data (Hauck *et al.* 1998) and field mapping (Lee *et al.* 2002). Although the data are from further west, the STD and KD are drawn to be consistent with our overall interpretation. The Kangmar dome likely formed during Pulse III.

Davidson *et al.* 1997; Chakungal *et al.* 2003). These high temperatures contributed to the observed inverted metamorphic field gradient of central Bhutan (Swapp & Hollister 1991), and heat from the leucogranite intrusions and migmatite of the hanging wall locally upgraded the metamorphic assemblages of the footwall of the Kakhtang thrust (Davidson *et al.* 1997).

According to Grujic *et al.* (2002), the Kakhtang thrust is coeval with normal shearing along the STD, which occurred at 10–11 Ma, based on cooling ages of micas in top-to-north mylonitized leucogranite (Maluski *et al.* 1988; Edwards & Harrison 1997; Wu *et al.* 1998). The thrusting appears to have folded leucogranite bodies in its footwall that have solidification ages as young as 13 Ma (Grujic *et al.* 2002). The timing of the thrusting, 10–11 Ma, is compatible with the cooling dates reported for the GHS in Bhutan (Maluski *et al.* 1988; Ferrara *et al.* 1991; Stüwe & Foster 2001). The thrust led to a doubling of the thickness of the exposed GHS in central Bhutan (Figs 1 & 5). The hanging wall of the Kakhtang thrust may be a segment split off from down the dip of the original channel as a result of folding of the channel roof (Grujic *et al.* 2002) or a result of extrusion of a dome formed in the channel (Grujic *et al.* 2004). The episode of rapid exhumation of the GHS appears to have preceded the out-of-sequence Kakhtang thrust by 1–2 million years.

Discussion and conclusions

Hollister & Crawford (1986) proposed that partial melting would lead to brief periods of high strain rates localized where the crust was weakened by melt. Rosenberg & Handy (2005) have recently

proposed a mechanism for melt-dependent weakening that produces a dramatic strength drop during the early stages of melting to an *c*. 7% melt fraction, which is caused by the increase of melt interconnectivity. They further propose that a second, less pronounced strength drop occurs at higher melt fractions and corresponds to the breakdown of the crystal framework at the commonly referred to 'rheologically critical melt percentage'. The tectonic implications of melt weakening have been expanded upon by Hollister (1993) who noted the linkage between melt weakening and rapid exhumation recorded in metamorphic rock in four orogens, including the Himalaya. With the channel flow model, the connection between melt weakening and focused surface erosion may provide an explanation for occurrences of decompression at high temperature recorded in metamorphic rocks.

Because the rocks in the footwall of the MCT in Bhutan were metamorphosed at pressures as high as those that are recorded within the hanging wall, a portion of the footwall must be considered to be included with the channel. In addition, pervasive top-to-south ductile shearing is recognized for at least 2 km into the LHS below the MCT (Grujic *et al.* 1996). Clearly, this portion of the channel did not contain melt during the channel flow. Thus, the channel must be considered as having rheologies ranging from those appropriate for ductile flow in greenschist-facies rocks to those for reaction-enhanced weakening to those with small amounts of melt to those for largely liquid mushes. The lower channel boundary is defined rheologically, not lithologically, and it lies within the LHS. The rheologically defined upper channel boundary lies within or at the top of the Chekha Formation rather than at the STD. This may explain the presence of two levels of normal-fault-geometry ductile shear zones (Fig. 1) – the lower between the Chekha (equivalent to the Everest Series) and the underlying GHS, and the upper between the Chekha and the overlying Tethyan Series – and is at least geometrically similar to the structural situation observed in the Mount Everest massif (Searle *et al.* 2003, 2006) and in the Annapurna–Manaslu region (Searle & Godin 2003; Godin *et al.* 2006).

If channel flow is a major process in the Miocene and younger history of the Himalayan orogen, then, for central Bhutan, the existence of the out-of-sequence Kakhtang thrust and the dramatic exhumation of the GHS and the LHS call for additional pulses of channel flow (Fig. 5). The first pulse lasted from 22 to 16 Ma and was bounded approximately by the MCT and the lower STD. It was followed by a second pulse that terminated by about 13 Ma; this one, which is cryptic, was bounded below by the MBT, and above by a detachment about where the later Kakhtang thrust occurred. By 10 Ma, the third pulse, now recognized in the hanging wall of the Kakhtang thrust, had finished, and all the rocks now exposed at the surface had cooled to below 250°C as documented by the mica cooling ages and by low temperature geochronology (e.g. Grujic *et al.* 2004).

Given the interplay between time, cooling, and changes in rheology of the channel, discontinuities in the pattern of channel flow seem likely. As the initial melt-bearing channel cools and the head begins to solidify, the head becomes a plug that impedes further flow. Continuation of the processes that drive channel flow will lead to new channels that will push through or break around the plug.

We were assisted in the field by C. Daniel, R. Parrish, K. Klepeis, R. Kuendig, C. Hollister, T. Pavlis, S. Schmidt, T. Dorjee and K.S. Ghalley; discussions with these colleagues contributed significantly to the content of this paper. Reviews by R. Brown, M. Brown and R. Law led to significant improvements in the manuscript. L. Hollister was supported by grants from the US National Science Foundation. D. Grujic acknowledges support from the Canadian Institute for Advanced Research (CIAR) and the Natural Sciences & Engineering Research Council of Canada. We are very grateful to Frank and Lisina Hoch, and their Bhutanese friends, for helping make our fieldwork possible.

References

BEAUMONT, C., JAMIESON, R. A., NGUYEN, M. H. & LEE, B. 2001. Himalayan tectonics explained by extrusion of a low-viscosity crustal channel coupled to focused surface denudation. *Nature*, **414**, 738–742.

BEAUMONT, C., JAMIESON, R. A., NGUYEN, M. H. & MEDVEDEV, S. 2004. Crustal channel flows: 1. Numerical models with applications to the tectonics of the Himalayan–Tibetan orogen. *Journal of Geophysical Research*, **109**. DOI: 10.1029/2003JB002809.

BHARGAVA, O. N. 1995. *The Bhutan Himalaya: A Geological Account*. Geological Survey of India, Special Publication, **39**.

BRUNEL, M. & KIENAST, J.-R. 1986. Etude pétrostructurale des chevauchements ductiles himalayens sur la transversale de l'Everest-Makalu (Népal oriental). *Canadian Journal of Earth Sciences*, **23**, 1117–1137.

BURCHFIEL, B. C., CHEN, Z., HODGES, K. V., LIU, Y., ROYDEN, L. H., DENG, C. & XU, J. 1992. *The South Tibetan detachment system, Himalayan orogen: Extension contemporaneous with and parallel to shortening in a collisional mountain belt*. Geological Society of America Special Paper, **269**.

CAROSI, R. C., MONTOMOLI, C., RUBATTO, D. & VISONA, D. 2006. Normal-sense shear zones in the core of the Higher Himalayan Crystallines (Bhutan Himalayas): evidence for extrusion?

In: LAW, R. D., SEARLE, M. P. & GODIN, L. (eds) *Channel Flow, Ductile Extrusion and Exhumation in Continental Collision Zones*. Geological Society, London, Special Publications, **268**, 425–443.

CASTELLI, D. & LOMBARDO, B. 1988. The Gophu La and Western Lunana granites: Miocene muscovite leucogranites of the Bhutan Himalaya. *Lithos*, **21**, 211–225.

CATLOS, E. J., HARRISON, T. M., KOHN, M. J., GROVE, M., RYERSON, F. J., MANNING, C. E. & UPRETI, B. N. 2001. Geochronologic and thermobarometric constraints on the evolution of the Main Central Thrust, central Nepal Himalaya. *Journal of Geophysical Research, B, Solid Earth and Planets*, **106**, 16,177–16,204.

CATLOS, E. J., DUBEY, C. S., HARRISON, T. M. & EDWARDS, M. A. 2004. Late Miocene movement within the Himalayan Main Central Thrust shear zone, Sikkim, north-east India. *Journal of Metamorphic Geology*, **22**, 207–226.

CHAKUNGAL, J., GRUJIC, D., DOSTAL, J. & GHALLEY, K. S. 2003. Towards understanding eohimalayan tectonics: Do gabbroic cumulates and ultramafics of the Bhutan Himalaya hold the clues? *In*: *18th Himalaya–Karakoram–Tibet Workshop Abstract Volume*, ETH, Zurich.

DANIEL, C. G., HOLLISTER, L. S., PARRISH, R. R. & GRUJIC, D. 2003. Exhumation of the Main Central Thrust from lower crustal depths, eastern Bhutan Himalaya. *Journal of Metamorphic Geology*, **21**, 317–334.

DASGUPTA, S., GANGULY, J. & NEOGI, S. 2004. Inverted metamorphic sequence in the Sikkim Himalayas: crystallization history, P-T gradient and implications. *Journal of Metamorphic Geology*, **22**, 395–412.

DAVIDSON, C., GRUJIC, D., HOLLISTER, L. S. & SCHMID, S. M. 1997. Metamorphic reactions related to decompression and synkinematic intrusion of leucogranite, High Himalayan Crystallines, Bhutan. *Journal of Metamorphic Geology*, **15**, 593–612.

EDWARDS, M. A. & HARRISON, T. M. 1997. When did the roof collapse? Late Miocene north-south extension in the high Himalaya revealed by Th-Pb monazite dating of the Khula Kangri granite. *Geology*, **25**, 543–546.

EDWARDS, M. A., KIDD, W. S. F., LI, J., YUE, Y. & CLARK, M. 1996. Multi-stage development of the southern Tibet detachment system near Khula Kangri. New data from Gonto La. *Tectonophysics*, **260**, 1–19.

FERRARA, G., LOMBARDO, B., TONARINI, S. & TURI, B. 1991. Sr, Nd and O isotopic characterisation of the Gophu La and Gumburanjun leucogranites (High Himalaya). *Schweizerische Mineralogische und Petrographische Mitteilungen*, **71**, 35–51.

GANGULY, J., DASGUPTA, S., CHENG, W. & NEOGI, S. 2000. Exhumation history of a section of the Sikkim Himalayas, India; records in the metamorphic mineral equilibria and compositional zoning of garnet. *Earth and Planetary Science Letters*, **183**, 471–486.

GANSSER, A. 1983. *Geology of the Bhutan Himalaya*. Birkhäuser Verlag, Basel.

GODIN, L., GLEESON, T. P., SEARLE, M. P., ULLRICH, T. D. & PARRISH, R. R. 2006. Locking of southward extrusion in favour of rapid crustal-scale buckling of the Greater Himalayan Sequence, Nar valley, central Nepal. *In*: LAW, R. D., SEARLE, M. P. & GODIN, L. (eds) *Channel Flow, Ductile Extrusion and Exhumation in Continental Collision Zones*. Geological Society, London, Special Publications, **268**, 269–292.

GRASEMANN, B., FRITZ, H. & VANNAY, J.-C. 1999. Quantitative kinematic flow analysis from the Main Central Thrust Zone (NW-Himalaya, India): implications for a decelerating strain path and the extrusion of orogenic wedges. *Journal of Structural Geology*, **21**, 837–853.

GRUJIC, D., CASEY, M., DAVIDSON, C., HOLLISTER, L. S., KUNDIG, R., PAVLIS, T. & SCHMID, S. 1996. Ductile extrusion of the Higher Himalayan Crystalline in Bhutan: evidence from quartz microfabrics. *Tectonophysics*, **260**, 21–43.

GRUJIC, D., HOLLISTER, L. & PARRISH, R. 2002. Himalayan metamorphic sequence as an orogenic channel: insight from Bhutan. *Earth and Planetary Science Letters*, **198**, 177–191.

GRUJIC, D., BEAUMONT, C., JAMIESON, R. A. & NGUYEN, M. H. 2004. Extruded domes in the Greater Himalayan Sequence: model predictions and possible examples. *In*: SEARLE, M., LAW, R. & GODIN, L. (eds), *Channel Flow, Ductile Extrusion and Exhumation of Lower-mid Crust in Continental Collision Zones*, *Abstract Volume*, Geological Society, London.

HARRIS, N. & MASSEY, J. 1994. Decompression and anatexis of Himalayan metapelites. *Tectonics*, **13**, 1537–1546.

HARRIS, N., CADDICK, M., KOSLER, J., GOSWAMI, S., VANCE, D. & TINDLE, A. G. 2004. The pressure-temperature-time path of migmatites from the Sikkim Himalaya. *Journal of Metamorphic Geology*, **22**, 249–264.

HAUCK, M. L., NELSON, K. D., BROWN, L. D., ZHAO, W. & ROSS, A. R. 1998. Crustal structure of the Himalayan orogen at $\sim 90^{\circ}$ east longitude from Project INDEPTH deep reflection profiles. *Tectonics*, **17**, 481–500.

HODGES, K. V. 2000. Tectonics of the Himalaya and southern Tibet from two perspectives. *GSA Bulletin*, **112**, 324–350.

HOLLISTER, L. S. 1993. The role of melt in the uplift and exhumation of orogenic melts. *Chemical Geology*, **108**, 31–48.

HOLLISTER, L. S. & CRAWFORD, L. M. 1986. Melt-enhanced deformation: a major tectonic process. *Geology*, **14**, 558–561.

HUBBARD, M. S. 1989. Thermobarometric constraints on the thermal history of the Main Central Thrust Zone and Tibetan Slab, eastern Nepal Himalaya. *Journal of Metamorphic Geology*, **7**, 19–30.

INGER, S. & HARRIS, N. B. W. 1992. Tectonothermal evolution of the High Himalayan crystalline sequence, Langtang Valley, northern Nepal. *Journal of Metamorphic Geology*, **10**, 439–452.

JAMIESON, R. A., BEAUMONT, C., MEDVEDEV, S. & NGUYEN, M. H. 2004. Crustal channel flows: 2. Numerical models with implications for metamorphism in the Himalayan-Tibetan Orogen. *Journal of Geophysical Research*, **109**. DOI: 10.1029/2003JB002811.

JAMIESON, R. A., BEAUMONT, C., NGUYEN, M. H. & GRUJIC, D. 2006. Provenance of the Greater Himalayan Sequence and associated rocks: predictions of channel flow models. *In*: LAW, R. D., SEARLE, M. P. & GODIN, L. (eds) *Channel Flow, Ductile Extrusion and Exhumation in Continental Collision Zones*. Geological Society, London, Special Publications, **268**, 165–182.

LEE, J., DINKLAGE, W. S., WANG, Y. & WAN, J. L. 2002. *Geology of Kangmar dome, south Tibet*. Geological Society of America Map and Chart Series, **MCH090**.

LOMBARDO, B. & ROLFO, F. 2000. Two contrasting eclogite types in the Himalayas: implications for the Himalayam orogeny. *Journal of Geodynamics*, **30**, 37–60.

MACFARLANE, A. M. 1995. An evaluation of the inverted metamorphic gradient at Langtang National Park, Central Nepal Himalaya. *Journal of Metamorphic Geology*, **13**, 595–612.

MALUSKI, H., MATTE, P., BRUNEL, M. & XIAO, X. 1988. Argon 39–argon 40 dating of metamorphic and plutonic events in the North and High Himalaya belts (southern Tibet, China). *Tectonics*, **7**, 299–326.

NELSON, K. D., ZHAO, W., BROWN, L. D. *ET AL.* 1996. Partially molten middle crust beneath southern Tibet; synthesis of Project INDEPTH results. *Science*, **274**, 1684–1688.

NEOGI, S., DASGUPTA, S. & FUKUOKA, M. 1998. High P-T polymetamorphism, dehydration melting, and generation of migmatites and granites in the Higher Himalayan Crystalline Complex, Sikkim, India. *Journal of Petrology*, **39**, 61–99.

ROSENBERG, C. L. & HANDY, M. R. 2005. Experimental deformation of partially melted granite revisited: implications for the continental crust. *Journal of Metamorphic Geology*, **23**, 19–28 DOI: 10.1111/j.1525-1314.2005.00555.x.

SEARLE, M. P. & GODIN, L. 2003. The South Tibetan Detachment and the Manaslu Leucogranite: A structural reinterpretation and restoration of the Annapurna-Manaslu Himalaya, Nepal. *Journal of Geology*, **111**, 505–523.

SEARLE, M. P. & SZULC, A. G. 2005. Channel flow and ductile extrusion of the high Himalayan slab-the Kangchenjunga-Darjeeling profile, Sikkim Himalaya. *Journal of Asian Earth Sciences*, **25**, 173–185.

SEARLE, M. P., SIMPSON, R. L., LAW, R. D., PARRISH, R. R. & WATERS, D. J. 2003. The structural geometry, metamorphic and magmatic evolution of the Everest massif, High Himalaya of Nepal-South Tibet. *Journal of the Geological Society*, London, **160**, 345–366.

SEARLE, M. P., LAW, R. D. & JESSUP, M. J. 2006. Crustal structure, restoration and evolution of the Greater Himalaya in Nepal–South Tibet: implications for channel flow and ductile extrusion of the middle crust. *In*: LAW, R. D., SEARLE, M. P. & GODIN, L. (eds) *Channel Flow, Ductite Extrusion and Exhumation in Continental Collision Zones*. Geological Society, London, Special Publications, **268**, 355–378.

SPEAR, F. S., KOHN, M. J. & CHENEY, J. T. 1999. P-T paths from anatectic pelites. *Contributions to Mineralogy and Petrology*, **134**, 17–32.

STÜWE, K. & FOSTER, D. 2001. $^{40}Ar/^{39}Ar$, temperature and fission-track constraints on the age and nature of metamorphism around the main central thrust in the eastern Bhutan Himalaya. *Journal of Asian Earth Sciences*, **19**, 85–95.

SWAPP, S. M. & HOLLISTER, L. S. 1991. Inverted metamorphism within the Tibetan slab of Bhutan: evidence for a tectonically transported heat-source. *Canadian Mineralogist*, **29**, 1019–1041.

THIMM, K. A., PARRISH, R. R., HOLLISTER, L. S., GRUJIC, D., KLEPEIS, K., DORJI, T. & KRÖNER, A. 1999. New U-Pb data from the Lesser and Greater Himalayan Sequences in Bhutan. *10th meeting of the European Union of Geosciences, Strasbourg, France. Journal of Conference Abstracts*, **4**, 57.

VANNAY, J.-C. & GRASEMANN, B. 1998. Inverted metamorphism in the High Himalaya of Himachal Pradesh (NW India): Phase equilibria versus thermobarometry. *Schweizerische Mineralogische und Petrographische Mitteilungen*, **78**, 107–132.

VANNAY, J.-C. & HODGES, K. V. 1996. Tectonometamorphic evolution of the Himalayan metamorphic core between Annapurna and Dhaulagiri, central Nepal. *Journal of Metamorphic Geology*, **14**, 635–656.

VANNAY, J.-C., GRASEMANN, B., RAHN, M., FRANK, W., CARTER, A., BAUDRAZ, V. & COSCA, M. 2004. Miocene to Holocene exhumation of metamorphic crustal wedges in the NW Himalaya: Evidence for tectonic extrusion coupled to fluvial erosion. *Tectonics*, **23**, DOI: 10.1029/2002TC001429.

WIESMAYR, G., EDWARDS, M. A., MEYER, M., KIDD, W. S. F., LEBER, D., HAUSLER, D. & WANGDA, D. 2002. Evidence for steady fault-accommodation strain in the High Himalaya: progressive fault rotation of the southern Tibet detachment system in NW Bhutan. *In*: DE MEER, S., DRURY, M. R., DE BRESSER, J. H. P. & PENNOCK, G. M. (eds) *Deformation Mechanisms, Rheology and Tectonics: Current Status and Future Perspectives.* Geological Society, London, Special Publications, **200**, 371–386.

WU, C., NELSON, K. D., WORTMAN, G., *ET AL.* 1998. Yadong cross structure and South Tibetan detachment in the east central Himalaya (89°–90°E). *Tectonics*, **17**, 28–45.

ZHANG, H., HARRIS, N., PARRISH, R. *ET AL.* 2004. Causes and consequences of protracted melting of the mid-crust exposed in the North Himalayan antiform. *Earth and Planetary Science Letters*, **228**, 195–212.